# Redox Behavior of Edge-Shared Bioctahedral $[Re_2(\mu\text{-}NCS)_2(NCS)_8]^{3-}$ and Its Relationship to the Direct Metal−Metal-Bonded Ion $[Re_2(NCS)_8]^{2-}$: A Spectroelectrochemical Study

**Robin J. H. Clark* and David G. Humphrey***

Christopher Ingold Laboratories, University College London, 20 Gordon Street, London WC1H 0AJ, United Kingdom

*Received August 24, 1995*[⊗]

Electrochemical and spectroelectrochemical studies have shown that the edge-shared bioctahedral $[Re_2(\mu\text{-}NCS)_2(NCS)_8]^{3-}$ anion can be reversibly oxidized and reduced (in one-electron steps) with retention of structure to give the even electron species $[Re_2(\mu\text{-}NCS)_2(NCS)_8]^{2-}$ and $[Re_2(\mu\text{-}NCS)_2(NCS)_8]^{4-}$. A second oxidation of $[Re_2(\mu\text{-}NCS)_2(NCS)_8]^{3-}$ is however only partially reversible, the $[Re_2(\mu\text{-}NCS)_2(NCS)_8]^{1-}$ ion being of limited stability. Further irreversible oxidation of this latter species can be achieved in what appears to be a ligand-based process yielding cyanide-containing species. An irreversible two-electron reduction of $[Re_2(\mu\text{-}NCS)_2(NCS)_8]^{4-}$ culminates in structural rearrangement to the direct metal−metal-bonded ion $[Re_2(NCS)_8(NCS)_2]^{6-}$, as shown by voltammetric and spectroelectrochemical measurements. Re-oxidation of $[Re_2(NCS)_8(NCS)_2]^{6-}$ results in the quantitative reformation of the edge-shared structure $[Re_2(\mu\text{-}NCS)_2(NCS)_8]^{4-}$. This reversible structural interconversion occurs in both noncoordinating and coordinating solvents, as well as in the presence of a high concentration of free $Cl^-$. The redox behavior of $[Re_2(NCS)_8]^{2-}$ has also been reinvestigated, and the relationship between the direct metal−metal-bonded and edge-shared bioctahedral structures established. Oxidation of $[Re_2(NCS)_8]^{2-}$ at room temperature results in the formation of $[Re_2(\mu\text{-}NCS)_2(NCS)_8]^{2-}$ and $NCS^-$-depleted products. $[Re_2(NCS)_8]^{2-}$ reacts immediately with 2 mol equiv of $NCS^-$ to give $[Re_2(\mu\text{-}NCS)_2(NCS)_8]^{4-}$, which is susceptible to aerial oxidation. At low temperature, however, the one-electron oxidation and reduction of $[Re_2(NCS)_8]^{2-}$ become reversible on the time scale of the IR spectroelectrochemical experiment, such that $[Re_2(NCS)_8]^{1-}$ and $[Re_2(NCS)_8]^{3-}$ have been characterized *in situ*. Further reduction of $[Re_2(NCS)_8]^{3-}$ to $[Re_2(NCS)_8]^{4-}$ is partially reversible under these conditions thus permitting characterization of the latter species.

## Introduction

The redox activity of metal−metal (M−M) bonded dirhenium complexes has proved to be one of the most interesting aspects of the chemistry of this general class of compound.[1] Of those structures formed by M−M-bonded complexes, there are two which are more commonly encountered among dirhenium systems, the double-bridged edge-shared bioctahedron (**I**, ESBO)

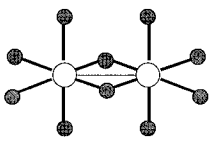

**I**

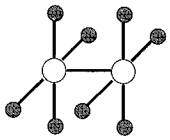

**II**

and the classical unsupported M−M-bonded structure (**II**). The consequences of electron transfer in complexes of these structural types are numerous. For instance the reduction of $[Re_2X_8]^{2-}$ can be achieved chemically with a variety of reagents, of which phosphines have been extensively used.[2−5] Upon reduction the substitution of halide by phosphine takes place, resulting in the formation of mixed halide−phosphine complexes of stoichiometry $[Re_2X_5(PR_3)_3]$ or $[Re_2X_4(PR_3)_4]$, depending upon the reaction conditions and the identity of the phosphine. The chemical oxidation of $[Re_2X_8]^{2-}$ (by $X_2$) can also be achieved,[6] culminating in a structural change, with the formation of the triple-bridged face-shared bioctahedral complex $[Re_2(\mu\text{-}X)_3X_6]^{1-}$.[7]

These are some of the many examples of redox reactions in which the final product has adopted a structure or composition different from that of the starting complex. Equally interesting, however, are cases where the overall features of the structure are preserved following electron transfer; the redox product may have undergone some changes in bond lengths and bond angles, but overall the essential features of the structure are retained. For example the electron-rich $[Re_2Cl_4(PMe_2Ph)_4]$ can be oxidized in two sequential one-electron steps to give $[Re_2Cl_4(PMe_2Ph)_4]^+$ and $[Re_2Cl_4(PMe_2Ph)_4]^{2+}$, both of which have been isolated and characterized by X-ray crystallography and shown to retain the parent structure.[8] Examples such as these provide an opportunity to examine M−M bonding as a function of electron population of the molecular orbital (MO) manifold.

As part of a study concerned with the consequences of electron transfer in bimetallic transition metal complexes, the redox behavior of ESBO $[Re_2(\mu\text{-}NCS)_2(NCS)_8]^{3-}$ has been

* Author to whom correspondence should be addressed.

[⊗] Abstract published in *Advance ACS Abstracts,* March 1, 1996.

(1) Cotton, F. A.; Walton, R. A. *Multiple Bonds Between Metal Atoms*, 2nd ed.; Clarendon Press: Oxford, U.K., 1993; pp 62−80.
(2) Cotton, F. A.; Frenz, B. A.; Ebner, J. R.; Walton, R. A. *J. Chem. Soc., Chem. Commun.* **1974**, 4−5.
(3) Ebner, J. R.; Walton, R. A. *Inorg. Chim. Acta* **1975**, *14*, L45−L46.
(4) Ebner, J. R.; Walton, R. A. *Inorg. Chem.* **1975**, *14*, 1987−1992.
(5) Glicksman, H. D.; Walton, R. A. *Inorg. Chem.* **1978**, *17*, 3197−3202.
(6) Bonati, F.; Cotton, F. A. *Inorg. Chem.* **1967**, *6*, 1353−1356.
(7) Cotton, F. A.; Ucko, D. A. *Inorg. Chim. Acta* **1972**, *6*, 161−172.
(8) Cotton, F. A.; Dunbar, K. R.; Falvello, L. R.; Tomas, M; Walton, R. A. *J. Am. Chem. Soc.* **1983**, *105*, 4950−4954.
(9) Best, S. P.; Clark, R. J. H.; Humphrey, D. G. *Inorg. Chem.* **1995**, *34*, 1013−1014.
(10) The $[Re_2(\mu\text{-}NCS)_2(NCS)_8]^{3-}$ anion, hereinafter designated $[Re_2(NCS)_{10}]^{3-}$, was originally formulated as $[Re_2(\mu\text{-}CO)_2(NCS)_{10}]^{3-}$,[11] on the basis of microanalytical data and the existence of two strong bands in the infrared spectrum at 1920 and 1889 $cm^{-1}$, thought to arise from bridging carbonyl groups. Not until 1979 was the true identity of the complex established,[12] when an X-ray crystallographic study revealed an ESBO structure with solely N-bound bridging $NCS^-$.

0020-1669/96/1335-2053$12.00/0 

investigated.[9,10] Like many ESBO dirhenium compounds,[13−25] the aforementioned complex has been found to display extensive redox chemistry in nonaqueous solvents; a series of sequential one-electron processes was observed, in addition to an overall two-electron process. Each of these processes has been examined by *in situ* spectroelectrochemical measurements, which reveal that both the one-electron oxidized and one-electron reduced products are remarkably stable and retain the ESBO structure. Further redox changes generate species which are more reactive, in particular structural rearrangement to an unsupported direct M−M-bonded complex occurs upon two-electron reduction of $[Re_2(NCS)_{10}]^{4-}$. In the course of these studies the redox behaviors of $[Re_2(NCS)_8]^{2-}$ and the simple monomeric $[Re(NCS)_6]^{2-}$ ion have also been examined. The results of these investigations, some of which have been communicated previously,[9] are described here.

## Experimental Section

**Materials.** $(^nBu_4N)_2[Re_2Cl_8]$[26,27] and $(^nBu_4N)_2[Re_2(NCS)_8]$[11] were prepared by literature procedures. $^nBu_4NOH$ (40% aqueous solution), $^nBu_4NNCS$, and $^nBu_4NCl$ were purchased from Aldrich. All other solvents and reagents were of analytical grade and used as received unless stated otherwise.

$(^nBu_4N)_3[Re_2(NCS)_{10}]$ was synthesized by minor modification to the original procedure of Cotton *et al.*[11] $(^nBu_4N)_2[Re_2Cl_8]$ (0.20 g, 0.18 mmol) and NaNCS (0.17 g, 0.21 mmol) were combined in a Schlenk flask and dissolved in 15.0 mL of acetone. The mixture was stirred for 2 h at room temperature and then filtered in air through a bed of Celite to remove NaCl. The solvent was removed from the filtrate *in vacuo*, and the resulting residue was stirred in absolute ethanol. A dark green microcrystalline precipitate formed, which was collected by filtration, washed with diethyl ether, and dried *in vacuo*. Microanalytical and spectroscopic data for this product were consistent with those for $(^nBu_4N)_3[Re_2(NCS)_{10}]$. Anal. Calcd (%) for $C_{58}H_{108}N_{13}S_{10}Re_2$: C, 41.5; H, 6.5; N, 10.8; S, 19.1. Found: C, 41.3; H, 6.1; N, 10.6; S, 19.2. IR (KBr): $\nu_{CN}$ region, 2072, 2052, 2036 (sh), 1918, 1882 $cm^{-1}$. Far-IR (paraffin wax): 483, 471, 442, 323, 294, 277, 260 $cm^{-1}$. Prolonged cooling of the filtrate from $(^nBu_4N)_3[Re_2(NCS)_{10}]$ gave a very small quantity of $(^nBu_4N)_2[Re(NCS)_6]$.

**Electrochemical Measurements.** Voltammetric experiments utilized a PAR 174A polargraphic analyzer and a PAR 175 waveform generator, in conjunction with Bryans Instruments 60000 Series X-Y/t chart recorder. Cyclic (CV) and differential pulse voltammetry (DPV) were performed using a conventional one-compartment, 3-electrode cell, the electrodes being a platinum bead working-electrode, a platinum bar auxiliary electrode, and a AgCl/Ag reference electrode calibrated against the ferrocenium/ferrocene $(Fe(Cp)_2^{+/0})$ couple (+0.55 V). Rotating disk voltammetry (RDV) employed a Metrohm Model 628-50 platinum rotating disk electrode. Bulk electrosynthesis was carried out in a two-compartment cell, with the platinum basket working electrode and AgCl/Ag reference electrode separated from the platinum auxiliary electrode by a double-fritted salt bridge. The charge transferred during a bulk electrosynthesis was measured with a Thompson Electrochem Model CM8 digital coulometer. Cooling of the solutions for low-temperature electrochemistry was achieved by immersion of the electrochemical cell in the appropriate solvent/dry ice slush bath. The temperature of the solution within the electrochemical cell was measured directly by a Comark digital thermometer.

Dichloromethane was predried over KOH and then distilled from $CaH_2$ just before use. Acetonitrile was predried over 4A molecular sieves and then distilled under nitrogen in turn from anhydrous $AlCl_3$, $KMnO_4/Li_2CO_3$, $KHSO_4$, and $CaH_2$, collecting the central fraction (∼75%) each time. A final distillation from $CaH_2$ was performed just prior to use. Tetrahydrofuran was predried over Na wire and then distilled under nitrogen from Na/K alloy just before use. *n*-Butyronitrile was predried over 4A molecular sieves and then vacuum distilled from $CaH_2$, collecting the middle fraction (∼75%) and storing under nitrogen over 4A molecular sieves.

The supporting electrolyte, tetra-*n*-butylammonium hexafluorophosphate ($^nBu_4NPF_6$), was prepared by neutralizing a 40% aqueous solution of tetra-*n*-butylammonium hydroxide with concentrated hexafluorophosphoric acid (*CAUTION: Very corrosive. Use in a fume hood only. Wear necessary protective clothing*). The crude electrolyte was washed extensively with distilled water and recrystallized (twice) from hot absolute ethanol. The purified electrolyte was then dried *in vacuo* at 100 °C for 24 h. Tetra-*n*-butylammonium perchlorate, $^nBu_4NClO_4$, was similarly prepared using perchloric acid (*note acid warnings above*), taking care to wash the crude electrolyte thoroughly to remove all traces of acid. Purification was achieved by recrystallization from hot absolute ethanol (twice) and by drying *in vacuo*, first at room temperature for 24 h and then at 50 °C for 24 h. Only small quantities of $^nBu_4NClO_4$ were dried at any one time.

Solutions for electrochemistry or spectroelectrochemistry were 0.5 mol $dm^{-3}$ in electrolyte for dichloromethane, 0.1 mol $dm^{-3}$ for acetonitrile and *n*-butyronitrile, and 0.25 mol $dm^{-3}$ for tetrahydrofuran. All electrolyte solutions were deoxygenated with solvent-saturated nitrogen prior to the addition of the complex to the cell.

**Spectroelectrochemical Measurements.** Infrared (IR) spectroelectrochemical experiments were carried out using an infrared reflection−absorption spectroscopic (IRRAS) cell mounted on a modified Specac specular reflectance attachment[28] located in the sample compartment of a dry-air purged Nicolet Magna 750 FTIR spectrometer. The electrode arrangement consisted of a highly polished platinum disk working electrode (5 mm diameter), a platinum gauze auxiliary electrode, and a platinum wire pseudoreference electrode. All spectroelectrochemical experiments were performed by stepping to a potential ($E_{app}$) *ca.* 0.2 V past the appropriate $E_{1/2}$ and collecting single-scan IR spectra (resolution = 1.0 $cm^{-1}$) as a function of time. Electrolyses were performed with a Bank POS 73 potentiostat.

Ultraviolet/visible (UV/vis) spectroelectrochemical experiments were carried out in a cryostated optically transparent thin-layer electrolysis (OTTLE) cell,[29] positioned in the sample compartment of a Perkin-Elmer Lambda 5 spectrophotometer. Contained in the OTTLE cell were a platinum gauze working electrode (*ca.* 75% transmission), a platinum wire auxiliary electrode, and a AgCl/Ag reference electrode. Electrolyses were performed with a Bank POS 73 potentiostat. Near-infrared (near-IR) spectra of electrogenerated species were collected using an analogous OTTLE cell arrangement in conjuction with a Perkin-Elmer Lambda 9 spectrophotometer, at the Research School of Chemistry, Australian National University.

(11) Cotton, F. A.; Robinson, W. R.; Walton, R. A.; Whyman, R. *Inorg. Chem.* **1967**, *6*, 929−935.
(12) Cotton, F. A.; Davison, A.; Ilsley, W. H.; Trop, H. S. *Inorg. Chem.* **1979**, *18*, 2719−2723.
(13) Barder, T. J.; Cotton, F. A.; Lewis, D.; Schwotzer, W.; Tetrick, S. M.; Walton, R. A. *J. Am. Chem. Soc.* **1984**, *106*, 2882−2891.
(14) Dunbar, K. R.; Powell, D.; Walton, R. A. *J. Chem. Soc., Chem. Commun.* **1985**, 114−116.
(15) Dunbar, K. R.; Powell, D.; Walton, R. A. *Inorg. Chem.* **1985**, *24*, 2842−2846.
(16) Cotton, F. A.; Dunbar, K. R.; Favello, L. R.; Walton, R. A. *Inorg. Chem.* **1985**, *24*, 4180−4187.
(17) Cotton, F. A.; Dunbar, K. R. *Inorg. Chem.* **1987**, *26*, 1305−1309.
(18) Anderson, L. B.; Cotton, F. A.; Dunbar, K. R.; Favello, L. R.; Price, A. C.; Reid, A. H.; Walton, R. A. *Inorg. Chem.* **1987**, *26*, 2717−2725.
(19) Fanwick, P. E.; Price, A. C.; Walton, R. A. *Inorg. Chem.* **1987**, *26*, 3920−3926.
(20) Esjornson, D.; Derringer, D. R.; Fanwick, P. E.; Walton, R. A. *Inorg. Chem.* **1989**, *28*, 2821−2829.
(21) Qi, J.; Fanwick, P. E.; Walton, R. A. *Inorg. Chem.* **1990**, *29*, 457−462.
(22) Qi, J.; Fanwick, P. E.; Walton, R. A. *Polyhedron* **1990**, *9*, 565−571.
(23) Fanwick, P. E.; Qi, J.; Schrier, P. W.; Walton, R. A. *Inorg. Chem.* **1992**, *31*, 258−262.
(24) Schrier, P. W.; Fanwick, P. E.; Walton, R. A. *Inorg. Chem.* **1992**, *31*, 3929−3933.
(25) Murray, H. H.; Wei, L.; Sherman, S. E.; Greaney, M. A.; Eriksen, K. A.; Carstensen, B.; Halbert, T. R.; Stiefel, E. I. *Inorg. Chem.* **1995**, *34*, 841−853.
(26) Barder, T. J.; Walton, R. A. *Inorg. Chem.* **1982**, *21*, 2510−2511.
(27) Barder, T. J.; Walton, R. A. *Inorg. Synth.* **1985**, *23*, 116−118.
(28) Best, S. P.; Clark, R. J. H.; Cooney, R. P.; McQueen, R. C. S. *Rev. Sci. Instrum.* **1987**, *58*, 2071−2074.
(29) Duff, C. M.; Heath, G. A. *Inorg. Chem.* **1991**, *30*, 2528−2535.

**Table 1.** IR and UV/vis Spectroscopic Data

| complex | infrared band max, $\nu_{CN}/cm^{-1}$ [a] dichloromethane | acetonitrile | tetrahydrofuran | electronic band max/$cm^{-1}$ ($\epsilon_{max}/M^{-1}\ cm^{-1}$)[b] |
|---|---|---|---|---|
| $[Re_2(NCS)_{10}]^{1-}$ | 1970 (m), 1825 (m) | *c* | *c* | *d* |
| $[Re_2(NCS)_{10}]^{2-}$ | 2062 (s), ~2045 (sh), 2022 (s), 1876 (m) | 2059 (s), ~2045 (sh), 2020 (s), 1878 (m) | 2060 (s), 2044 (s), 2017 (s), 1880 (m) | 40 700 (112 800), 21 700 (87 900), ~19 000 (sh), 14 200 (12 800) |
| $[Re_2(NCS)_{10}]^{3-}$ | 2111 (w), 2078 (s), 2058 (s), 1922 (m), 1885 (m) | 2078 (s), 2054 (s), 1926 (m), 1887 (m) | 2108 (w), 2077 (s), 2056 (s), 1923 (m), 1887 (m) | 41 100 (106 300), 23 400 (62 900), ~21 000 (sh), ~14 600 (sh) |
| $[Re_2(NCS)_{10}]^{4-}$ | 2099 (s), 2087 (s), 1933 (m) | 2097 (s), 2084 (s), 1935 (m) | 2098 (s), 2084 (s), 1934 (m) | 43 300 (103 500), 36 500 (68 500), 30 000 (29 700), 25 700 (43 400), 17 500 (8300) |
| $[Re_2(NCS)_8(NCS)_2]^{6-}$ | 2077 (s), ~2055−2058 (sh) | 2075 (s), 2059 (m) | 2075 (s), ~2060−2055 (sh) | 39 500 (141 600), 34 000 (66 300), 16 800 (3000), 14 000 (4000), 10 700 (4500) |
| $[Re_2(NCS)_8]^{1-}$ | | | 2013 (s), 1959 (m) | *e* |
| $[Re_2(NCS)_8]^{2-}$ | | | 2099 (w), 2051 (s), 1959 (w) | *e* |
| $[Re_2(NCS)_8]^{3-}$ | | | ~2109 (w), 2079 (s), ~1960 (w) | *e* |
| $[Re_2(NCS)_8]^{4-}$ | | | 2079 (m) | |

[a] Collected in an IRRAS cell at 253 K, in the solvent stated with the appropriate concentration of $^nBu_4NPF_6$ electrolyte (see Experimental Section). Qualitative intensities, s = strong, m = medium, w = weak, sh = shoulder. [b] Collected in an OTTLE cell in 0.5 mol $dm^{-3}$ $^nBu_4NPF_6/CH_2Cl_2$ at 233 K. [c] In acetonitrile or tetrahydrofuran the $[Re_2(NCS)_{10}]^{2-/1-}$ oxidation is not observed prior to an irreversible multi-electron process. [d] The $[Re_2(NCS)_{10}]^{1-}$ species proved to be insufficiently stable for electrogeneration in the OTTLE cell. [e] See ref 32.

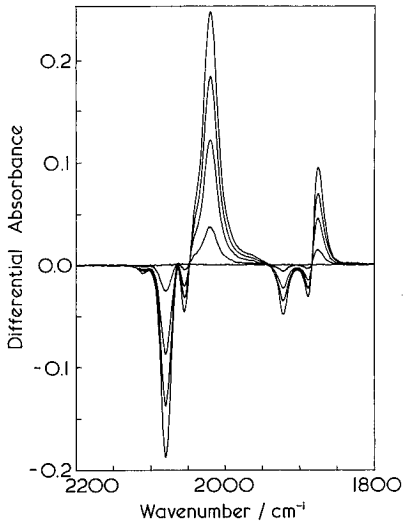


**Figure 1.** Changes in the IR difference spectra accompanying the $[Re_2(NCS)_{10}]^{3-/2-}$ oxidation, recorded at room temperature in an IRRAS cell, in 0.5 mol $dm^{-3}$ $^nBu_4NPF_6$/dichloromethane.

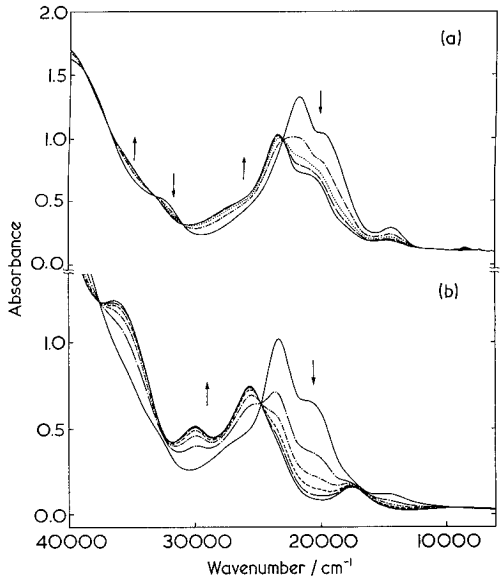


**Figure 2.** UV/vis spectral changes accompanying (a) the re-reduction of $[Re_2(NCS)_{10}]^{2-}$ following exhaustive oxidation of $[Re_2(NCS)_{10}]^{3-}$ and (b) $[Re_2(NCS)_{10}]^{3-/4-}$ reduction, recorded in an OTTLE cell, in 0.5 mol $dm^{-3}$ $^nBu_4NPF_6$/dichloromethane at 233 K.

## Results

**$(^nBu_4N)_3[Re_2(NCS)_{10}]$. Dichloromethane/$^nBu_4NPF_6$.** The CV and DPV of $(^nBu_4N)_3[Re_2(NCS)_{10}]$ revealed five well-defined processes, *i.e.* three oxidations and two reductions.[9] The first oxidation and first reduction occur at moderate potentials ($E_{1/2}$ = +0.46, 0.00 V, respectively) and are voltammetrically reversible with constant $\Delta E_p$ for scan rates 50−1000 mV $s^{-1}$ and $i_{pr}/i_{pf} = 1.0$. The potential vs current characteristics of these couples implies a one-electron process in each case, which was confirmed by coulometry. The $[Re_2(NCS)_{10}]^{3-/2-}$ oxidation and $[Re_2(NCS)_{10}]^{3-/4-}$ reduction were probed by IR and UV/vis spectroelectrochemical techniques. The changes in the IR difference spectra (1800−2200 $cm^{-1}$) accompanying one-electron oxidation of $[Re_2(NCS)_{10}]^{3-}$ are shown in Figure 1, and the results are summarized with those of the $[Re_2(NCS)_{10}]^{3-/4-}$ reduction in Table 1. In each case the spectral changes occurred with maintenance of isosbestic points and the quantitative reappearance of the starting spectrum was observed upon switching the potential of the working electrode to a rest potential after oxidation or reduction.

The IR spectrum of $[Re_2(NCS)_{10}]^{3-}$ consists of two bands at 2078 and 2058 $cm^{-1}$, assigned to $\nu_{CN}$ of terminal $NCS^-$, and two others at 1922 and 1885 $cm^{-1}$, assigned to $\nu_{CN}$ of the solely N-bound bridging $NCS^-$.[12] On oxidation the $\nu_{CN}$ bands moved to lower wavenumber and on reduction to higher wavenumber.[9] The average of the terminal bands shifted by 25 $cm^{-1}$ on oxidation and by 33 $cm^{-1}$ on reduction. The two bridging bands in $[Re_2(NCS)_{10}]^{3-}$ collapse to yield a single band for both of the even electron systems. The magnitude of these shifts in $\nu_{CN}$ is similar to that observed upon one-electron reduction of $[Re(NCS)_6]^{2-}$ (see below), and the direction is consistent with the $\sigma/\pi$ donor properties of $NCS^-$.

The stabilities of $[Re_2(NCS)_{10}]^{2-}$ and $[Re_2(NCS)_{10}]^{4-}$ were further highlighted by the room-temperature electrogeneration of these species in an OTTLE cell, where electrolysis times are generally at least 1 order of magnitude longer than in an IRRAS cell. The results are listed in Table 1. The electronic spectrum of $[Re_2(NCS)_{10}]^{3-}$ is dominated by several intense, overlapping absorptions in the region of 18 000−28 000 $cm^{-1}$ ($\nu_{max}$ = 23 300 $cm^{-1}$), which show some solvent dependence. Upon oxidation the absorption manifold was shifted to lower wavenumber (Figure 2a), while on reduction the manifold shifted to higher wavenumber (Figure 2b). The odd-electron $[Re_2(NCS)_{10}]^{3-}$ species also has a weak near-IR band around 7500 $cm^{-1}$, which moves to 8400 $cm^{-1}$ upon oxidation, and ~7000 $cm^{-1}$ upon reduction, although in the last case the band

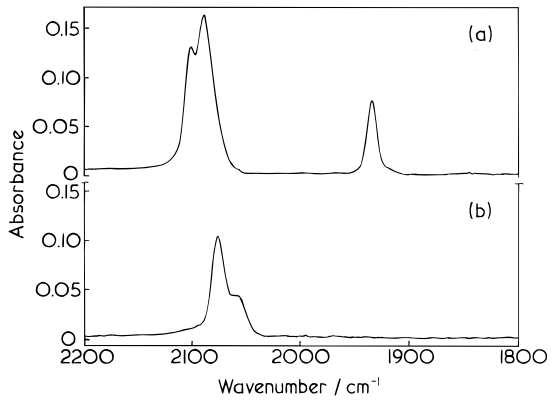


**Figure 3.** (a) IR spectrum of $[Re_2(NCS)_{10}]^{4-}$, electrogenerated at $E_{app} = -0.5$ V, in 0.5 mol dm$^{-3}$ $^n$Bu$_4$NPF$_6$/dichloromethane at 233 K. (b) Final IR spectrum after reduction of $[Re_2(NCS)_{10}]^{4-}$ at $E_{app} = -1.4$ V, in 0.5 mol dm$^{-3}$ $^n$Bu$_4$NPF$_6$/dichloromethane at 233 K.

is very weak and its wavenumber difficult to determine accurately. These bands are broad in comparison to single-ion type transitions.

Further oxidation of $[Re_2(NCS)_{10}]^{2-}$ can be achieved in what is best described as a partially reversible process ($E_{1/2} = +1.38$ V), with $i_{pc}/i_{pa} < 1.0$. Lowering the temperature of the solution (213 K) did not improve the reversibility of the $[Re_2(NCS)_{10}]^{2-/1-}$ couple, but it did permit partial characterization of the $[Re_2(NCS)_{10}]^{1-}$ species by IR spectroscopy. Oxidation of $[Re_2(NCS)_{10}]^{2-}$ at +1.4 V in the IRRAS cell led to the growth of bands at 1970 and 1825 cm$^{-1}$, at the expense of those from $[Re_2(NCS)_{10}]^{2-}$. The electrolysis proceeded to approximately 50% completion before the breakdown of isosbestic points occurred, consistent with the partial reversibility observed in the CV. Continuation of the electrolysis past this point did not permit complete regeneration of the $[Re_2(NCS)_{10}]^{2-}$ spectrum.

Continuation of the anodic scan past the $[Re_2(NCS)_{10}]^{2-/1-}$ oxidation revealed a further irreversible oxidation, with $E_{pa} \sim +1.5$ V. After electrogeneration of a solution of $[Re_2(NCS)_{10}]^{2-}$, the potential of the working electrode was stepped to +1.6 V, which led to significantly different spectral changes from those observed for the $[Re_2(NCS)_{10}]^{2-/1-}$ oxidation. The bands characteristic of $[Re_2(NCS)_{10}]^{2-}$ at 2062, 2022, and 1876 cm$^{-1}$ collapsed, with the growth of a feature at 1890 cm$^{-1}$ (and shoulder ~1905 cm$^{-1}$) and another strong, broad band centered at 2215 cm$^{-1}$. These spectral changes are irreversible. Since the $[Re_2(NCS)_{10}]^{2-/1-}$ and further oxidations were not chemically reversible on the time scale of the IR spectroelectrochemical experiment, no attempt was made to study these processes by UV/vis spectroscopy in the OTTLE cell.

The second reduction of $[Re_2(NCS)_{10}]^{3-}$, at $E_{pc} = -1.31$ V, was irreversible for scan rates 100−1000 mV s$^{-1}$. RDV and coulometry revealed that the irreversible reduction involved two-electrons overall. After scanning over the $[Re_2(NCS)_{10}]^{4-/6-}$ reduction, an additional process was detected on the return scan, which was not present when the scan was reversed prior to reduction. A multiple scan revealed that this coupled process has some reversibility, which suggests that some chemical process may follow electron transfer. The $[Re_2(NCS)_{10}]^{4-/6-}$ reduction remained irreversible at low temperature (213 K), but at this temperature, the coupled process became very broad (large $\Delta E_p$).

The $[Re_2(NCS)_{10}]^{4-/6-}$ reduction was probed spectroscopically. The changes in the IR spectrum accompanying the two-electron reduction of $[Re_2(NCS)_{10}]^{4-}$ (Figure 3a) at −1.4 V and 233 K occurred in two distinct phases, the first of which was very rapid and involved the nonisosbestic collapse of the bands

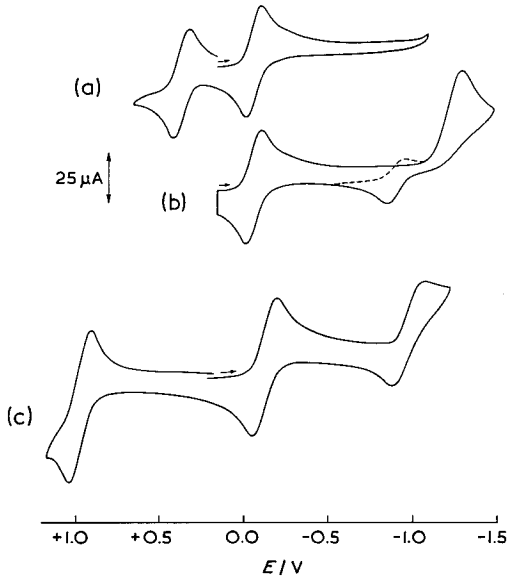


**Figure 4.** Cyclic voltammetry (a, b) of $(^n$Bu$_4$N$)_3[Re_2(NCS)_{10}]$ and (c) of $(^n$Bu$_4$N$)_2[Re_2(NCS)_8]$, recorded in 0.25 mol dm$^{-3}$ $^n$Bu$_4$NPF$_6$/tetrahydrofuran at room temperature. Scan rate = 100 mV s$^{-1}$.

at 2099, 2087, and 1933 cm$^{-1}$. Then, with the electrolysis essentially complete, the second phase of changes took place over a period of ~30 min. A slow series of minor spectral changes culminated in the relatively simple IR spectrum shown in Figure 3b, with a strong band at 2077 cm$^{-1}$ and a shoulder in the region 2055−2058 cm$^{-1}$. In accordance with the proposed EC type behavior, re-oxidation was not observed until $E_{app} = -0.5$ V, whereupon quantitative regeneration of the $[Re_2(NCS)_{10}]^{4-}$ spectrum occurred, albeit very slowly. Similarly the UV/vis spectrum of the fully reduced species was obtained by two-electron reduction of $[Re_2(NCS)_{10}]^{4-}$ in an OTTLE cell at 233 K. The final spectrum was dominated by two bands with maxima at 33 970 and 39 500 cm$^{-1}$. Several weak bands in the region 10 000−20 000 cm$^{-1}$ were also observed.

**Acetonitrile/$^n$Bu$_4$NPF$_6$ and Tetrahydrofuran/$^n$Bu$_4$NPF$_6$.** The CV of $(^n$Bu$_4$N$)_3[Re_2(NCS)_{10}]$ in acetonitrile or tetrahydrofuran (Figure 4) revealed some minor differences from those recorded in dichloromethane. The $E_{1/2}$ positions of the reversible couples were somewhat solvent dependent, and the $[Re_2(NCS)_{10}]^{2-/1-}$ oxidation was not observed prior to an irreversible multi-electron wave (at $E_{app} > +1.4$ V). The $[Re_2(NCS)_{10}]^{4-/6-}$ reduction remained irreversible, and the species formed subsequently was observed in each case. The IR spectral changes associated with each redox step were virtually identical to those obtained in dichloromethane, although some small solvent dependence of the peak positions was observed.

**Dichloromethane/$^n$Bu$_4$NX (X$^-$ = NCS$^-$, Cl$^-$).** The voltammetry of $(^n$Bu$_4$N$)_3[Re_2(NCS)_{10}]$ was also examined in dichloromethane/$^n$Bu$_4$NPF$_6$ containing ~0.05 mol dm$^{-3}$ $^n$Bu$_4$NNCS. The anodic window was limited to ~+0.6 V; thus, only the first oxidation of $[Re_2(NCS)_{10}]^{3-}$ was observed prior to the onset of oxidation of free NCS$^-$. The cathodic response of $[Re_2(NCS)_{10}]^{3-}$ was unchanged even with relatively high concentrations of free NCS$^-$ (0.5 mol dm$^{-3}$). The second two-electron reduction of $[Re_2(NCS)_{10}]^{z-}$ remained irreversible, and the product subsequently formed and detected at −0.64 V ($E_{pa}$) was again observed.

Similarly the voltammetry of $(^n$Bu$_4$N$)_3[Re_2(NCS)_{10}]$ was recorded in dichloromethane/$^n$Bu$_4$NCl (0.1 mol dm$^{-3}$), the anodic cutoff in this case being ~+0.8 V. The cathodic voltammetry was again unchanged from that obtained in

dichloromethane/$^n$Bu$_4$NPF$_6$. The low-temperature (233 K) reduction of $[Re_2(NCS)_{10}]^{4-}$ in the IRRAS cell at $E_{app} = -1.4$ V produced a spectrum identical to that obtained with $^n$Bu$_4$NPF$_6$ electrolyte, and re-oxidation at $E_{app} = -0.5$ V again resulted in the quantitative re-formation of $[Re_2(NCS)_{10}]^{4-}$.

**($^n$Bu$_4$N)$_2$[Re$_2$(NCS)$_8$]. Dichloromethane/Acetonitrile/$^n$Bu$_4$NPF$_6$ or *n*-Butyronitrile/$^n$Bu$_4$NPF$_6$.** The voltammetry of ($^n$Bu$_4$N)$_2$[Re$_2$(NCS)$_8$] has been noted previously,[30,31] most recently by Heath and Raptis who characterized $[Re_2(NCS)_8]^{1-}$ and $[Re_2(NCS)_8]^{3-}$ by low-temperature UV/vis/near-IR spectroelectrochemical measurements.[32] While the $[Re_2(NCS)_8]^{2-/1-}$ and $[Re_2(NCS)_8]^{2-/3-}$ couples are voltammetrically reversible at room temperature, chemical reversibility on the UV/vis spectroelectrochemical time scale was only achieved by performing the electrolysis in *n*-butyronitrile at ~215 K.

The one-electron oxidation and one-electron reduction of $[Re_2(NCS)_8]^{2-}$ were first probed by IR spectroscopy at room temperature. Not surprisingly, both processes were irreversible, and in the case of the $[Re_2(NCS)_8]^{2-/1-}$ oxidation, one of the products was identified. Oxidation of a dichloromethane/acetonitrile solution of $[Re_2(NCS)_8]^{2-}$ in the IRRAS cell clearly revealed the formation of $[Re_2(NCS)_{10}]^{2-}$, as shown by the growth of bands at 2023 and 1876 cm$^{-1}$. The latter can be assigned to $\nu_{CN}$ of the solely N-bound bridging NCS$^-$ of $[Re_2(NCS)_{10}]^{2-}$, while the former is one of two $\nu_{CN}$ bands from terminal NCS$^-$ groups. The second of the terminal bands, at 2062 cm$^{-1}$, is obscured by the presence of additional bands in the region around 2050−2060 cm$^{-1}$; these are attributed to NCS$^-$-depleted products. Similar results were obtained in *n*-butyronitrile at room temperature. Cooling the dichloromethane/acetonitrile solution to 233 K improved the stability of the redox products, $[Re_2(NCS)_8]^{1-}$ and $[Re_2(NCS)_8]^{3-}$, but still the one-electron processes were not fully reversible.

**Tetrahydrofuran/$^n$Bu$_4$NPF$_6$.** The oxidized and reduced species displayed considerably greater stability in tetrahydrofuran than in the other solvents tried. At 253 K both the one-electron oxidation and reduction were chemically reversible on the time scale of the IRRAS experiment, thus permitting collection of the IR spectra of $[Re_2(NCS)_8]^{1-}$ and $[Re_2(NCS)_8]^{3-}$ (Table 1). The changes in the IR spectra accompanying the oxidation and reduction are presented in Figure 5 (parts a and b). The direction and magnitude of the shifts in $\nu_{CN}$ are similar to those observed for the ESBO $[Re_2(NCS)_{10}]^{z-}$.

The enhanced stability of $[Re_2(NCS)_8]^{3-}$ in tetrahydrofuran enabled the quasi-reversible $[Re_2(NCS)_8]^{3-/4-}$ reduction to be probed spectroscopically. Reduction in the IRRAS cell (at ~253 K) proceeded to *ca.* 50% completion before breakdown of the isosbestic points was observed. Continuation of the electrolysis past this point did not allow the starting spectrum of $[Re_2(NCS)_8]^{3-}$ to be regenerated quantitatively upon switching the potential of the working electrode. The most outstanding feature of the spectral changes accompanying the early phase of this electrolysis was the apparent lack of new band(s) attributable to $[Re_2(NCS)_8]^{4-}$. The spectral changes accompanying the reduction were also monitored in difference mode, so that any new features, however weak, could be observed readily. The band characteristic of $[Re_2(NCS)_8]^{3-}$ at 2079 cm$^{-1}$ simply decreased in intensity, as shown in Figure 6, with no other $\nu_{CN}$ bands of NCS$^-$ observed in the region 2300−1700 cm$^{-1}$. Similar IR spectral changes have been observed to accompany the $[Re(NCS)_6]^{3-/4-}$ reduction (see below).

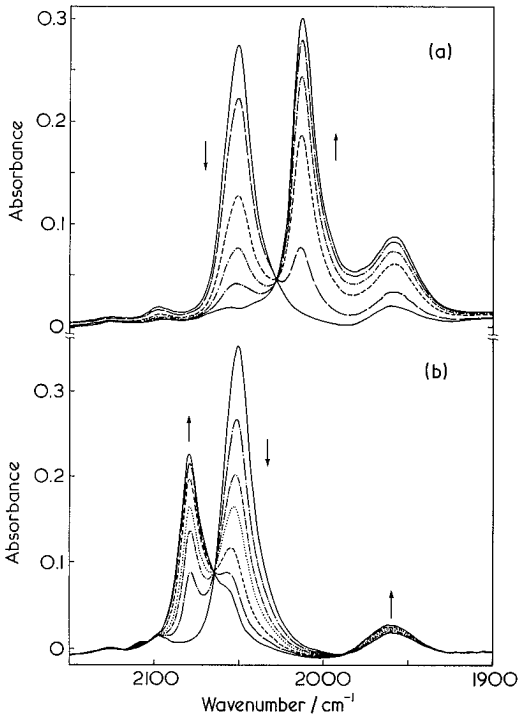


**Figure 5.** IR spectroelectrochemical monitoring of the (a) $[Re_2(NCS)_8]^{2-/1-}$ oxidation and (b) $[Re_2(NCS)_8]^{2-/3-}$ reduction, recorded in 0.25 mol dm$^{-3}$ $^n$Bu$_4$NPF$_6$/tetrahydrofuran at 253 K.

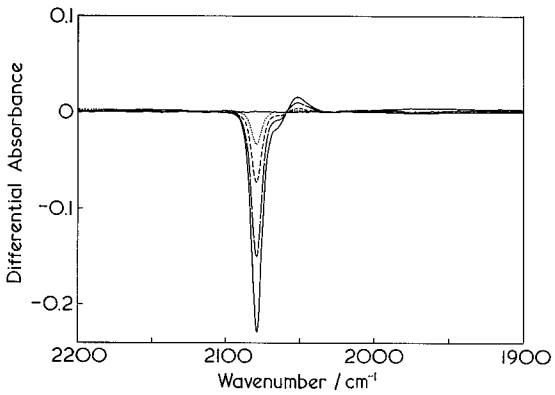


**Figure 6.** Changes in the IR difference spectrum during the initial stages of the $[Re_2(NCS)_8]^{3-/4-}$ reduction, recorded in 0.25 mol dm$^{-3}$ $^n$Bu$_4$NPF$_6$/tetrahydrofuran at 253 K. A negative absorbance of −0.22 for the band at 2079 cm$^{-1}$ corresponds to the loss of approximately 50% of the $[Re_2(NCS)_8]^{3-}$ originally present prior to commencement of the electrolysis.

**Dichloromethane/Acetonitrile Mixture/$^n$Bu$_4$NNCS.** The voltammetry of $[Re_2(NCS)_8]^{2-}$ was also examined in the presence of free NCS$^-$. A solution of $[Re_2(NCS)_8]^{2-}$ at room temperature reacted immediately with NCS$^-$, as shown by UV/vis spectroscopy. If, however, the $[Re_2(NCS)_8]^{2-}$ solution was cooled prior to addition of free NCS$^-$, then the rate at which the subsequent reaction took place was considerably reduced. The oxidation of NCS$^-$ occurs at potentials greater than ~+0.6 V; hence, the $[Re_2(NCS)_8]^{2-/1-}$ oxidation was not observed under these conditions. The potential of the $[Re_2(NCS)_8]^{2-/3-}$ reduction was essentially unmoved in the presence of free NCS$^-$.[33] With time processes attributable to a new species were

(30) Cotton, F. A.; Robinson, W. R.; Walton, R. A. *Inorg. Chem.* **1967**, *6*, 1257−1258.
(31) Hahn, J. E.; Nimry, T.; Robinson, W. R.; Salmon, D. J.; Walton, R. A. *J. Chem Soc., Dalton Trans.* **1978**, 1232−1236.
(32) Heath, G. A.; Raptis, R. G. *J. Am. Chem. Soc.* **1993**, *115*, 3768−3769.

(33) At low temperature $E_{1/2}$ for the $[Re_2(NCS)_8]^{3-/4-}$ reduction is difficult to determine accurately, due to extreme broadening (large $\Delta E_p$) of this couple.

observed (with $E_{1/2}$ ~+0.5, 0.0 V). The positions of these waves indicated the formation of ESBO $[Re_2(NCS)_{10}]^{z-}$. No other intermediate was observed voltammetrically. Conversion to $[Re_2(NCS)_{10}]^{z-}$ was complete after *ca.* 2 h at room temperature. RDV revealed that, for a solution protected by a nitrogen atmosphere, no electron transfer had taken place; *i.e.*, $[Re_2(NCS)_{10}]^{4-}$ had formed. However upon exposure of the solution to air, one-electron oxidation took place forming $[Re_2(NCS)_{10}]^{3-}$, as shown by RDV and UV/vis spectroscopy. Cotton *et al.* have noted the formation of $(^nBu_4N)_3[Re_2(NCS)_{10}]$ when $(^nBu_4N)_2[Re_2(NCS)_8]$ was treated with $^nBu_4NNCS$ in air,[34] and similarly the recrystallization of $(^nBu_4N)_2[Re_2(NCS)_8]$ from dichloromethane in air has been observed to yield $(^nBu_4N)_3[Re_2(NCS)_{10}]$.[35]

**$(^nBu_4N)_2[Re(NCS)_6]$. Dichloromethane/$^nBu_4NPF_6$.** The CV and DPV of $(^nBu_4N)_2[Re(NCS)_6]$ at 233 K revealed a reversible reduction ($[Re(NCS)_6]^{2-/3-}$), a quasi-reversible reduction ($[Re(NCS)_6]^{3-/4-}$), and a partially-reversible oxidation ($[Re(NCS)_6]^{2-/1-}$),[36] these findings being essentially in agreement with those obtained previously.[31] Each of the redox processes was examined by IR spectroelectrochemistry. The $[Re(NCS)_6]^{2-/3-}$ reduction was chemically reversible at room temperature, consistent with a previous report that the reduction of $(^nBu_4N)_2[Re(NCS)_6]$ with hydrazine hydrate gave air-sensitive $(^nBu_4N)_3[Re(NCS)_6]$.[37] The value of 2076 $cm^{-1}$ for $\nu_{CN}$ of $[Re(NCS)_6]^{3-}$ obtained here in solution by electrolysis in the IRRAS cell is in agreement with that found for $(^nBu_4N)_3[Re(NCS)_6]$ (KBr disk) at 2070 $cm^{-1}$.[37]

Following reduction to $[Re(NCS)_6]^{3-}$, the potential of the working electrode was stepped to −1.8 V to electrogenerate $[Re(NCS)_6]^{4-}$. The $\nu_{CN}$ band of $[Re(NCS)_6]^{3-}$ at 2076 $cm^{-1}$ simply decreased in intensity, leaving a far less intense band at the same wavenumber after exhaustive electrolysis. The lack of wavenumber change of the $\nu_{CN}$ band upon reduction to $[Re(NCS)_6]^{4-}$ may arise as a result of complementary $\sigma$ and $\pi$ bonding effects on the N−C−S and Re−N bonds with change in oxidation state, $Re^{III/II}$ $d^4/d^5$. The spectral changes with this second reduction were fully reversible, since returning the potential to $E_{app}$ = −0.5 V resulted in the quantitative re-formation of the $[Re(NCS)_6]^{3-}$ spectrum, and isosbestic points were maintained with each redox step. The $[Re(NCS)_6]^{2-/1-}$ oxidation was also examined, but conditions under which this process became chemically reversible were not discovered.

## Discussion

**Reversible Electron-Transfer in $[Re_2(NCS)_{10}]^{z-}$.** The changes in the $\nu_{CN}$ region of the IR spectrum upon one-electron oxidation or reduction are consistent with retention of the ESBO structure for $[Re_2(NCS)_{10}]^{z-}$ ($z$ = 2 or 4). The solely N-bound bridging $NCS^-$ is clearly retained for $z$ = 2 or 4, as shown by bands at 1876 and 1933 $cm^{-1}$, respectively. While the $[Re_2(NCS)_{10}]^{2-/1-}$ oxidation is not fully reversible, the IR spectral changes observed during the early phase of the electrolysis suggest the $[Re_2(NCS)_{10}]^{1-}$ anion also retains the parent ESBO structure, although it has only limited stability. The electron count through these series of changes ($z$ = 1−4) is summarized in Figure 7.

The X-ray crystal structure of $[Re_2(NCS)_{10}]^{3-}$ shows significant distortion away from an idealized ESBO structure, for which the Re−N−Re′ and N−Re−N′ bond angles would be equal to 90°.[38] The Re−N−Re′ and N−Re−N′ bond angles for $[Re_2(NCS)_{10}]^{3-}$ are 77 and 102°, respectively, suggesting the presence of a Re−Re bond (Re−Re = 2.613(1) Å). It therefore seems appropriate to describe the bonding within the parent $[Re_2(NCS)_{10}]^{3-}$ ion in terms of the MO scheme described previously for M−M-bonded ESBO complexes,[39,40] corresponding to an electronic configuration $(\sigma)^2(\pi)^2(\delta)^2(\delta^*)^1$. The identity of redox-active orbital is, however, somewhat uncertain, since theoretical studies have shown that, when the bridging ligands have orbitals of suitable symmetry to interact with the metal d orbtials, then re-ordering of $\delta$ and $\delta^*$ can occur. Should this occur, then the HOMO of $[Re_2(NCS)_{10}]^{3-}$ becomes $(\delta)^1$. Whatever the nature of the redox-active orbital, the $\delta$-bond is in general very weak for complexes of this structure and thus a change in the electron occupancy of the $\delta$ (or $\delta^*$) orbital is unlikely to perturb the metal-metal bond strength significantly; retention of the ESBO structure upon one-electron oxidation and reduction is therefore understandable. This in itself is good evidence for a $\delta$ or $\delta^*$ HOMO in $[Re_2(NCS)_{10}]^{3-}$. The recently solved X-ray crystal structure of $[Re_2(NCS)_{10}](BEDT\text{-}TTF)_2{\cdot}C_6H_5CN$ (containing $Re^{IV}_2$, $d^3d^3$)[41] reveals few if any changes in the structural dimensions of the $\{Re(\mu\text{-}NCS)_2Re\}^{6+}$ bridge.[42] These observations are in accord with the weak nature of the $\delta$ bond due to poor direct d-orbital overlap; the strength of the M−M bond in ESBO complexes is largely governed by the M−M $\sigma$-bond interaction.

Another pair of structurally characterized ESBO complexes are $[Re_2(\mu\text{-}Cl)_2(Cl_4)(\mu\text{-}dppm)_2]^+$ ($d^3d^4$) and $[Re_2(\mu\text{-}Cl)_2(Cl_4)$-

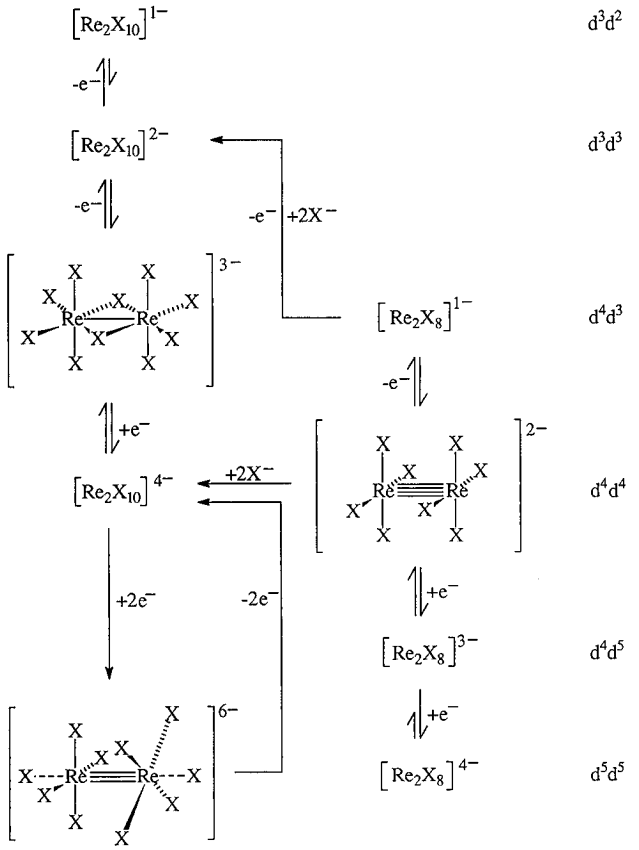


**Figure 7.** Summary scheme. X = $NCS^-$.

(34) Cotton, F. A.; Matusz, M. *Inorg. Chem.* **1987**, *26*, 3468−3472.
(35) Heath, G. A.; Raptis, R. G. Personal Communication.
(36) In dichloromethane/$^nBu_4NPF_6$ at 233 K: $[Re(NCS)_6]^{2-/3-}$, $E_{1/2}$ = −0.05 V, $\Delta E_p$ = 60 mV, $i_{pa}/i_{pc}$ = 1.0; $[Re(NCS)_6]^{3-/4-}$, $E_{1/2}$ = −1.43 V, $\Delta E_p$ = 120 mV, $i_{pa}/i_{pc}$ = 1.0; $[Re(NCS)_6]^{2-/1-}$, $E_{1/2}$ ~ +1.3 V, $\Delta E_p$ = 70 mV, $i_{pc}/i_{pa}$ < 1.0.
(37) Trop, H. S.; Davison, A.; Jones, A. G. *Inorg. Chim. Acta* **1981**, *54*, L61.
(38) Cotton, F. A. *Polyhedron* **1987**, *6*, 667−677.
(39) Shaik, S.; Hoffmann, R.; Fisel, C. R.; Summerville, R. H. *J. Am. Chem. Soc.* **1980**, *102*, 4555−4572.
(40) Poli, R.; Torralba, R. C. *Inorg. Chim. Acta* **1993**, *212*, 123−134.
(41) BEDT-TTF = bis(ethylenedithio)tetrafulvalene.
(42) Kepert, C. J.; Day, P. Personal Communication.

($\mu$-dppm)$_2$] ($d^4d^4$),[15] the former being isoelectronic with $[Re_2(NCS)_{10}]^{3-}$ and the latter with $[Re_2(NCS)_{10}]^{4-}$. Reduction of $[Re_2(\mu\text{-}Cl)_2(Cl_4)(\mu\text{-dppm})_2]^+$ (Re−Re = 2.68 Å) results in shortening of the Re−Re distance by some 0.07 Å, although the bridging dppm ligands may enforce some geometric constraints on the structure which overide or attenuate electronic effects to some extent. The authors concluded that the observed structural changes were consistent with strengthening of the M−M bond, as a consequence of filling of a $\delta$-bonding orbital; hence, the MO scheme (in order of increasing energy) is $\sigma < \pi < \delta^* < \delta < \pi^* < \sigma^*$.

The electronic spectra of bimetallic complexes, in particular the near-IR region in the case of dirhenium complexes, are potentially rich in information regarding the nature of the M−M interactions. The weak bands in the near-IR region can be assigned to transitions between metal-based MO, although more specific assignments are at present unwarranted. The visible spectra of $[Re_2(NCS)_{10}]^{z-}$ ($z = 2-4$) are likely to be dominated by ligand-to-metal charge-transfer (LMCT) transitions of the type $NCS^-$ ($2\pi$) to the metal-based MO manifold, similar in origin to those transitions that dominate the spectra of $[Re(NCS)_6]^{z-}$ ($z = 2$ or 3), $NCS^-$ ($2\pi$) to Re ($d\pi$).[43,44] While the electronic spectra of the latter are relatively simple,[45] the complexity of the $[Re_2(NCS)_{10}]^{z-}$ spectra can be attributed to the lower symmetry of this complex (ideally $D_{2h}$), with (in principle) LMCT from both the axial and equatorial terminal $NCS^-$ and also bridging $NCS^-$, the latter expected at higher energy than the former. The intense bands in the midvisible region of $[Re_2(NCS)_{10}]^{z-}$ also shift upon oxidation and reduction, in a manner consistent with the LMCT assignment of these transitions.

**Irreversible Electron Transfer in $[Re_2(NCS)_{10}]^{z-}$.** Oxidation of $[Re_2(NCS)_{10}]^{2-}$ at $E_{app} = +1.6$ V led to an unusual series of changes in the IR spectrum, culminating in the appearance of a relatively broad, strong band at 2215 cm$^{-1}$. The characteristics of this band (*i.e.* wavenumber and shape) are reminiscent of $\nu_{CN}$ of coordinated cyanide, such that ligand oxidation of coordinated $NCS^-$ to $CN^-$ may be occurring. The oxidation of N-bound $NCS^-$ to $CN^-$ has been noted previously.[46] A more systematic study of some rhenium cyanides is presently underway.[47]

The nature of the product formed upon the two-electron reduction of $[Re_2(NCS)_{10}]^{4-}$ was of considerable interest. The spectroscopic changes (both IR and UV/vis) which followed the reduction suggested major structural rearrangement of the ESBO. These results, and those from voltammetric studies, are consistent with the formation of a direct, unsupported M−M-bonded complex, $[Re_2(NCS)_8(NCS)_2]^{6-}$. The highly symmetrical structure of such a complex is in agreement with the relatively simple IR spectrum obtained after reduction, and the most intense $\nu_{CN}$ band at 2077 cm$^{-1}$ compares very closely with that of $[Re_2(NCS)_8]^{4-}$ ($\nu_{CN}$ at 2079 cm$^{-1}$). The shoulder at *ca.* 2055−2058 cm$^{-1}$ is assigned to weakly associated $NCS^-$ occupying the axial sites of the M−M-bonded structure (see later discussion). This new species, related to $[Re_2(NCS)_8]^{2-}$ by two one-electron oxidations, has a one-electron oxidation with $E_{1/2} \sim -0.67$ V (dichloromethane).[48] As expected, this occurs at almost exactly the same potential as $E_{1/2}$ for $[Re_2(NCS)_8]^{3-/4-}$ (−0.69 V).[49]

The UV/vis/near-IR spectrum of the reduced species is also consistent with the proposed $[Re_2(NCS)_8(NCS)_2]^{6-}$ formulation. The overall two-electron reduction of $[Re_2(NCS)_{10}]^{4-}$ results in a 10-electron system ($d^5d^5$) and an anticipated $(\sigma)^2(\pi)^4(\delta)^2(\delta^*)^2$ electronic configuration. Consequently the near-IR region of the electronic spectrum is expected to be featureless, as observed, since full occupation of the $\delta^*$ orbital removes the possibility of $\delta-\delta^*$ transitions, characteristic of $[Re_2(NCS)_8]^{z-}$ ($z = 1-3$).[32] The intense bands at >30 000 cm$^{-1}$ presumably have their origin in charge-transfer transitions, $NCS^-$ ($2\pi$) to $\pi^*$ of the metal-based MO manifold. A related M−M triple-bonded complex is $[Re_2(CH_3CN)_8(CH_3CN)_2]^{4+}$,[50] which has a staggered conformation and axial $CH_3CN$. The electronic spectra of $[Re_2(CH_3CN)_8(CH_3CN)_2]^{4+}$ and $[Re_2(NCS)_8(NCS)_2]^{6-}$ are remarkably similar, in that they both contain a number of very weak transitions in the visible region and two intense bands at higher energy.

Several alternative structures were considered to that proposed for $[Re_2(NCS)_8(NCS)_2]^{6-}$, but these were each discounted in turn. ESBO decahalodimetalate complexes, $[M_2(\mu\text{-}X)_2X_8]^{z-}$, have been observed to condense to triple-bridged face-shared bioctahedral (FSBO) nonahalodimetalates, $[M_2(\mu\text{-}X)_3X_6]^{z-}$, upon reduction.[51,52] In the present case, an absence of bands assignable solely to N-bound bridging $NCS^-$ rules out the formation of a triple-bridged face-shared structure upon reduction of $[Re_2(NCS)_{10}]^{4-}$. Furthermore a structural rearrangement of this kind, should it occur, necessarily involves the dissociation of $NCS^-$. The CV of $[Re_2(NCS)_{10}]^{3-}$ remained unchanged in the presence of free $NCS^-$, suggesting that a dissociative process does not accompany the reduction of $[Re_2(NCS)_{10}]^{4-}$. Similarly bridging of $NCS^-$ via N and S can also be discounted, as structures showing this bridging mode give rise to $\nu_{CN}$ in the region 2100−2150 cm$^{-1}$.[53]

The formation of monomeric complexes can also be discounted on the basis of spectroscopic evidence and the observation that upon re-oxidation at −0.50 V the $[Re_2(NCS)_{10}]^{4-}$ species re-forms quantitatively, in both dichloromethane and acetonitrile, and similarly in the presence of a high concentration of $Cl^-$. Should a coordinatively unsaturated fragment have been formed upon reduction of $[Re_2(NCS)_{10}]^{4-}$, through cleavage of the bimetallic ESBO structure into monomeric units,[54] then

(43) Gutterman, D. F.; Gray, H. B. *Inorg. Chem.* **1972**, *11*, 1727−1733.
(44) Gutterman, D. F.; Gray, H. B. *J. Am. Chem. Soc.* **1971**, *93*, 3364−3371.
(45) The electronic spectrum of $[Re(NCS)_6]^{2-}$ (acetonitrile solution) is dominated by a single band at 420 nm (23 800 cm$^{-1}$), while that of $[Re(NCS)_6]^{3-}$ (acetonitrile solution) has a band at 370 nm (27 000 cm$^{-1}$).[37]
(46) Newman, A. A., Ed. *Chemistry and Biochemistry of Thiocyanic Acid and its Derivatives*; Academic Press: London, 1975; pp 119−121 and references cited therein.
(47) Clark, R. J. H.; Humphrey, D. G. Work in progress.
(48) Depending upon the conditions under which the CV was performed (*i.e.* solvent and temperature), a second wave was at times also detected, almost coincident with the $[Re_2(NCS)_{10}]^{3-/4-}$ couple. This second wave is attributed to the $[Re_2(NCS)_8(NCS)_2]^{5-/4-}$ oxidation, at a very similar position to that of the $[Re_2(NCS)_8]^{2-/3-}$ process. Note that on the time scale of the CV experiment, the re-formation of $[Re_2(NCS)_{10}]^{4-}$ is not observed.
(49) The apparent insensitivity of the $[Re_2(NCS)_8]^{3-/4-}$ reduction potential to axial ligation of $NCS^-$ can be understood when the nature of the redox-active orbital is considered. The electron enters the $\delta^*$ orbital, which has little if any component available for overlap with the incoming axial ligand. The addition of $(^nBu_4N)_2[Re_2(NCS)_8]$ to a electrochemical solution of $(^nBu_4N)_3[Re_2(NCS)_{10}]$ revealed that the species produced after scanning over the $[Re_2(NCS)_{10}]^{4-/6-}$ reduction was detected at the same potential (within the resolution limits of CV) as the $[Re_2(NCS)_8]^{3-/4-}$ reduction, in all solvents used.
(50) Bernstein, S. N.; Dunbar, K. R. *Angew. Chem., Int. Ed. Engl.* **1992**, *31*, 1360−1362.
(51) Humphrey, D. G. Ph.D. Thesis, The Australian National University, 1992.
(52) Heath, G. A.; Humphrey, D. G. *J. Chem. Soc., Chem. Commun.* **1990**, 672− 674.
(53) Bailey, R. A.; Kozak, S. L.; Michelsen, T. W.; Mills, W. N. *Coord. Chem. Rev.* **1971**, *6*, 407−445.

either a coordinating solvent or free $Cl^-$ may have been expected to trap such a fragment and prevent re-formation of the ESBO structure.

**Mechanistic Considerations.** A concerted mechanism of the type discussed by Hoffmann *et al.* may account for the formation of $[Re_2(NCS)_8(NCS)_2]^{6-}$ from an ESBO structure.[39] Such a mechanism involves the breaking of two opposite Re−($\mu$-NCS) bonds, with concerted rotation about each of the axial SCN−Re−NCS axes. This has the effect of placing previously terminal $NCS^-$ groups in positions co-aligned with the Re−Re bond, and the previously bridging $NCS^-$ groups are found diagonally opposed across the unsupported Re−Re bond.[55] The spectral changes which accompany such an intramolecular process would, however, be expected to occur with isosbestic points. This is not the case, and so an additional process must also occur. For this we propose rotation about the M−M bond, since the $(\sigma)^2(\pi)^4(\delta)^2(\delta^*)^2$ electronic configuration effectively cancels out the weak $\delta$-bond, such that the structure is free to adopt either staggered, eclipsed, or intermediate conformations. This would explain the two stages of spectral changes observed in the formation of the final product and the lengthy time taken for the re-formation of the ESBO $[Re_2(NCS)_{10}]^{4-}$ structure. Overall, the redox reaction and rearrangement can be described more explicitly as an EECC mechanism, whereby two-electron reduction (EE) is followed by formation of the direct M−M bond and subsequent rotation about the M−M bond. This sequence of events is favored over the other obvious alternative, ECEC, given that the $[Re_2(NCS)_8]^{3-/4-}$ reduction was not fully reversible on the time scale of the spectroelectrochemical experiments.

We tentatively propose that $NCS^-$ remain weakly associated with the M−M-bonded $[Re_2(NCS)_8]^{4-}$ unit. Although the band in the region 2055−2058 $cm^{-1}$ could be assigned to free $NCS^-$, we instead attribute this to the axial $NCS^-$. Furthermore the re-formation of $[Re_2(NCS)_{10}]^{4-}$ following re-oxidation, in both coordinating and noncoordinating solvents and in the presence of high concentrations of $Cl^-$, suggests that the axial $NCS^-$ groups remain coordinated (albeit very weakly) to the $[Re_2(NCS)_8]^{4-}$ unit.

M−M bond lengths in Re−Re triple-bonded complexes typically lie in the range 2.25−2.30 Å.[56] The Re−Re distance in the parent $[Re_2(NCS)_{10}]^{3-}$ ion is 2.613 Å, and given that little change is expected in the dimensions of $\{Re(\mu\text{-}NCS)_2Re\}^{z+}$ upon reduction to $[Re_2(NCS)_{10}]^{4-}$ (see earlier discussion), then considerable contraction presumably occurs along the M−M vector with two-electron reduction. Attempts are presently underway to determine the structure of $[Re_2(NCS)_{10}]^{4-}$ and establish the precise dimensions of the $\{Re(\mu\text{-}NCS)_2Re\}^{4+}$ core prior to the formation of the unsupported M−M-bonded structure. Large changes in M−M distances in bimetallic complexes have previously been observed to accompany two-electron redox processes.[57−60]

The sequence of EC steps leading to the re-formation of $[Re_2(NCS)_{10}]^{4-}$ upon re-oxidation of $[Re_2(NCS)_8(NCS)_2]^{6-}$ appear different from those by which the latter is formed, since the oxidation of $[Re_2(NCS)_8(NCS)_2]^{6-}$ initially involves just one electron, as does the isovalent $[Re_2(NCS)_8]^{3-/4-}$ couple. $[Re_2(NCS)_{10}]^{4-}$ is detected as soon as the re-oxidation commences, although overall the quantitative reformation is slow. No intermediates are observed over this time such that the chemical rearrangement following the $[Re_2(NCS)_8(NCS)_2]^{6-/5-}$ oxidation and the further one-electron oxidation must all occur in another concerted process.

**Re-Examination of $[Re_2(NCS)_8]^{2-}$.** The formation of $[Re_2(NCS)_{10}]^{2-}$ upon oxidation of $[Re_2(NCS)_8]^{2-}$ at room temperature presumably occurs via an $NCS^-$ scavenging mechanism. Overall, two-electron oxidation occurs but, given that the first oxidation of $[Re_2(NCS)_8]^{2-}$ is known to be a one-electron process, an ECE mechanism is likely. The $[Re_2(NCS)_8]^{1-}$ strips 2 equiv of $NCS^-$ from other $[Re_2(NCS)_8]^{2-}$, forming $[Re_2(NCS)_{10}]^{3-}$, which at the potential of the $[Re_2(NCS)_8]^{2-/1-}$ oxidation ($E_{app} = +1.2$ V) is rapidly oxidized to $[Re_2(NCS)_{10}]^{2-}$. Halide scavenging mechanisms have previously been encountered in dirhenium chemistry and considered to account for the formation of $[Re_2(\mu\text{-}Cl)_3Cl)_6]^{1-}$ from $[Re_2Cl_8]^{2-}$ upon electrochemical oxidation of the latter at room temperature[61] and similarly the oxidative-induced conversion of $[Re_2Cl_4(dppm)_2]$ to $[Re_2Cl_5(dppm)_2]$[62] and then to ESBO $[Re_2(\mu\text{-}Cl)_2Cl_4(dppm)_2]$.[13] The $NCS^-$-depleted product(s) following the formation of $[Re_2(NCS)_{10}]^{2-}$ remain unidentified.

The facile conversion of $[Re_2(NCS)_8]^{2-}$ to $[Re_2(NCS)_{10}]^{4-}$ in the presence of free $NCS^-$ can be readily followed by CV. The rearrangement is essentially the reverse of that described above, with $NCS^-$ initially occupying the positions axial to the M−M bond, followed by formation of the double-bridged structure. The synthesis of $[Re_2(NCS)_{10}]^{3-}$ can therefore be readily understood, since the moderate potential required to oxidize $[Re_2(NCS)_{10}]^{4-}$ to $[Re_2(NCS)_{10}]^{3-}$ is in the range where oxygen can function as an oxidant. The reaction of phosphines ($PR_3$) with $[Re_2(NCS)_8]^{2-}$ to give $[Re_2(\mu\text{-}NCS)_2(NCS)_6(PR_3)_2]^{2-}$ are similarly rationalized in this way,[63] although interestingly the latter are thought to contain N- and S-bound bridging $NCS^-$, not solely N-bound $NCS^-$ as in the case of $[Re_2(NCS)_{10}]^{z-}$ ($z = 2-4$). These studies have further illustrated the close relationship between the direct M−M-bonded and ESBO structures. IR characterization of $[Re_2(NCS)_8]^{z-}$ ($z = 1-4$) has also been achieved, in tetrahydrofuran at low temperature, complementing the work of Heath and Raptis, who previously

(54) The ESBO structure could cleave either symmetrically or asymmetrically, *i.e.* form two $[Re(NCS)_5]^{3-}$ fragments or a $[Re(NCS)_6]^{4-}$ and $[Re(NCS)_4]^{2-}$ fragment. The two-band IR spectrum is not inconsistent with a five- coordinate trigonal bipyramidal structure ($D_{3h}$) in the case of the former, but such a species is likely to be highly reactive and achieve coordinative saturation in the presence of potential ligands (MeCN, $Cl^-$, $NCS^-$, *etc.*). Re-formation of the ESBO structure would then appear improbable. Asymmetric cleavage seems equally unlikely, in that $[Re(NCS)_6]^{4-}$ is known to be stable in dichloromethane at low temperature and, hence, upon re-oxidation would itself simply be oxidized to $[Re(NCS)_6]^{3-}$, readily identifiable in the IR spectrum ($\nu_{CN}$ = 2076 $cm^{-1}$). The $[Re(NCS)_4]^{2-}$ fragment, which may even form $[Re_2(NCS)_8]^{4-}$ in a strictly noncoordinating environment, is expected to behave in a similar manner to $[Re(NCS)_5]^{3-}$ in the presence of potential ligands.

(55) This mechanism, or variations thereof, is often used to describe the fluxional exchange of carbonyl groups in polynuclear metal carbonyl compounds. For a general discussion see: Cotton, F. A.; Wilkinson, G. *Advanced Inorganic Chemistry*, 5th ed.; John Wiley and Sons: New York, 1988; pp 1325−1327.

(56) Cotton, F. A.; Walton, R. A. *Multiple Bonds Between Metal Atoms*, 2nd ed.; Clarendon Press: Oxford, U.K., 1993; pp 72−73.

(57) Gennett, T.; Geiger, W. E.; Willett, B.; Anson, F. C. *J. Electroanal. Chem.* **1987**, *222*, 151−160.

(58) Smith, D. A.; Zhuang, B.; Newton, W. E.; McDonald, J. W.; Schultz, F. A. *Inorg. Chem.* **1977**, *16*, 2524−2531.

(59) Ginsburg, R. E.; Rothrock, R. K.; Finke, R. G.; Collman, J. P.; Dahl, L. F. *J. Am. Chem. Soc.* **1979**, *101*, 6550−6562.

(60) Collman, J. P.; Rothrock, R. K.; Finke, R. G.; Moore, E. J.; Rose-Munch, F. *Inorg. Chem.* **1982**, *21*, 146−156.

(61) Heath, G. A.; Raptis, R. G. *Inorg. Chem.* **1991**, *30*, 4106−4108.

(62) $[Re_2Cl_5(dppm)_2]$ complex has an end-capped direct M−M bonded structure, with two *trans* dppm ((diphenylphosphino)methane) ligands bridging the Re−Re bond and four $Cl^-$ occupying the other equatorial positions. The remaining $Cl^-$ is located in one of the axial positions collinear with the Re−Re bond: Cotton, F. A.; Shive, L. W.; Stults, B. R. *Inorg. Chem.* **1976**, *15*, 2239−2244.

(63) Nimry, T.; Walton, R. A. *Inorg. Chem.* **1977**, *16*, 2829−2834.

characterized $[Re_2(NCS)_8]^{z-}$ ($z = 1-3$) by UV/vis/near-IR spectroelectrochemical studies.

## Conclusion

The redox behavior of the ESBO $[Re_2(NCS)_{10}]^{3-}$ ion has been examined in detail and is summarized in Figure 7. Spectroelectrochemical investigations suggest the parent ESBO structure $[Re_2(NCS)_{10}]^{z-}$ is preserved for $z = 1$, 2, or 4, although $[Re_2(NCS)_{10}]^{1-}$ has only limited stability. Further oxidation of $[Re_2(NCS)_{10}]^{1-}$ can be achieved in what appears to be a ligand-based process, resulting in the formation of $CN^-$-containing species. Two-electron reduction of $[Re_2(NCS)_{10}]^{4-}$ results in a novel structural transformation, forming the direct M−M-bonded $[Re_2(NCS)_8(NCS)_2]^{6-}$. Overall this process is reversible, since re-oxidation of the latter re-forms $[Re_2(NCS)_{10}]^{4-}$ quantitatively. Additional studies on the quadruply metal−metal-bonded $[Re_2(NCS)_8]^{2-}$ ion have mapped out the intimate relationship between these structurally different dirhenium complexes. Furthermore this work has served to highlight the value of *in situ* spectroelectrochemical techniques for studying the redox chemistry of highly reactive transition metal complexes.

**Acknowledgment.** D.G.H. thanks the Royal Society for an Endeavour Fellowship and the Ramsay Memorial Fellowship Trust for a British Ramsay Fellowship. The authors also thank Dr. S. P. Best (University of Melbourne) and Dr. D. A. Tocher (University College London) for helpful discussion, Mr. C. J. Kepert and Prof. P. Day (Royal Institution) for the preliminary communication of X-ray structural data, and Dr. G. A. Heath (Australian National University) for making available the facilities used to collect electrogenerated near-IR spectra. The EPSRC and the University of London (CRF) are thanked for financial support.

IC9511276